

Modern Physics Letters A
 © World Scientific Publishing Company

Cosmic expansion and structure formation in running vacuum cosmologies

Spyros Basilakos*

*Research Center for Astronomy and Applied Mathematics, Academy of Athens
 Soranou Efessiou 4, 11527, Athens, Greece
 svasil@academyofathens.gr*

We investigate the dynamics of the FLRW flat cosmological models in which the vacuum energy varies with redshift. A particularly well motivated model of this type is the so-called quantum field vacuum, in which both kind of terms H^2 and constant appear in the effective dark energy density affecting the evolution of the main cosmological functions at the background and perturbation levels. Specifically, it turns out that the functional form of the quantum vacuum endows the vacuum energy of a mild dynamical evolution which could be observed nowadays and appears as dynamical dark energy. Interestingly, the low-energy behavior is very close to the usual Λ CDM model, but it is by no means identical. Finally, within the framework of the quantum field vacuum we generalize the large scale structure properties, namely growth of matter perturbations, cluster number counts and spherical collapse model.

Keywords: Cosmology; Dark Energy; Large Scale Structure.

PACS Nos.: 98.80.-k, 95.35.+d, 95.36.+x

1. Introduction

The statistical analysis of various cosmological data (SNIa, Cosmic Microwave Background-CMB, Baryonic Acoustic Oscillations-BAOs, Hubble parameter measurements etc) strongly suggests that we live in a spatially flat universe that consists of $\sim 4\%$ baryonic matter, $\sim 26\%$ dark matter and $\sim 70\%$ some sort of dark energy (hereafter DE) which is necessary to explain the accelerated expansion of the universe (see Refs.[1, 2] and references therein). Although there is a common agreement regarding the ingredients of the universe, there are different views concerning the possible physical mechanism which is responsible for the cosmic acceleration.

The simplest dark energy candidate corresponds to a cosmological constant. In the standard concordance Λ CDM model, the overall cosmic fluid contains baryons, cold dark matter plus a vacuum energy (cosmological constant), that appears to fit accurately the current observational data and thus provides an excellent scenario to describe the observed universe. However, the concordance model suffers from, among other, two fundamental problems: (a) *The fine tuning problem* i.e., the fact that

*email: svasil@academyofathens.gr

the observed value of the vacuum energy density ($\rho_\Lambda = \Lambda c^2/8\pi G \simeq 10^{-47} \text{ GeV}^4$) is many orders of magnitude below the value found using quantum field theory (QFT),³ and (b) *the coincidence problem*,⁴ i.e., the fact that the matter energy density and the vacuum energy density are of the same order just prior to the present epoch, despite the fact that the former is a rapidly decreasing function of time while the latter is stationary. Such problems have inspired many authors to propose alternative candidates to the concordance Λ CDM, such as general dark energy models and modifications of the theory of gravity (for review see Ref.[5]).

An alternative path that one can follow in order to alleviate the above problems is to consider a time varying vacuum, $\Lambda(t)$. Within this framework we do not need to include new fields in nature nor to modify the theory of General Relativity. In this cosmological scenario the dark energy equation of state parameter $w \equiv P_{DE}/\rho_{DE}$, is strictly equal to -1, but the vacuum energy density is not a constant but rather it is a function of the cosmic time. Note that there is an extensive (old^{6,8} and new⁹⁻¹⁴) literature in which the time-evolving vacuum has been phenomenologically modeled as a function of time in various possible ways, in particular, as a function of the Hubble parameter.

In this article we reconsider the so called quantum field vacuum (see next section). We would like to stress that this vacuum model was previously investigated by our team in many aspects. The layout of the article is the following. In section 2, we present the main cosmological ingredients of the quantum field vacuum model. In section 3 we provide the power spectrum and the linear growth of matter perturbations. In sections 4 and 5 we discuss the cluster number counts and the spherical collapse model. Finally, we draw our conclusions in section 6.

2. Background expansion - Observational constraints

The nature of the current vacuum model⁹⁻¹² is essentially connected with the renormalization group (RG) in quantum field theory (QFT). In this context, the evolution of the vacuum is written as

$$\Lambda(H) = \Lambda_0 + 3\nu(H^2 - H_0^2). \quad (1)$$

where $\Lambda_0 \equiv \Lambda(H_0) = 3\Omega_\Lambda H_0^2$ and ν is interpreted in the RG framework as a “ β -function” of QFT in curved spacetime, which determines the running of the cosmological constant. Regarding the dynamical role of ν it has been found that since $|\nu| \ll 1$ (for a recent discussion see Ref. [13] and references therein) at low redshifts the model becomes almost indistinguishable from the cosmic concordance model. In other words the ν -parameter endows the vacuum energy of a mild dynamical evolution which could be observed nowadays and appears as dynamical dark energy. The low-energy behavior is thus very close to the concordance model, but it is by no means identical.

Naturally, the next step here is to derive the Friedmann equations assuming of course a running vacuum. This procedure is perfectly allowed by the Cosmological

Principle embedded in the FLRW metric. In this context the Friedmann equations are written

$$8\pi G\rho_{\text{tot}} \equiv 8\pi G\rho_m + \Lambda = 3\left(\frac{\dot{a}}{a}\right) = 3H^2, \quad (2)$$

$$8\pi Gp_{\text{tot}} \equiv 8\pi Gp_m - \Lambda = -2\dot{H} - 3H^2 \quad (3)$$

where the overdot denotes derivative with respect to cosmic time t . Notice that the Bianchi identities that insure the covariance of the theory, pose an energy exchange between vacuum and matter for $G = \text{const}$.

$$\dot{\rho}_m + 3(1 + \omega_m)H\rho_m = -\dot{\rho}_\Lambda. \quad (4)$$

Combining equations (2), (3) and (4), we provide the basic differential equation that governs the dynamics of the Universe

$$\dot{H} + \frac{3}{2}(1 + \omega_m)H^2 = \frac{(1 + \omega_m)}{2}\Lambda(H). \quad (5)$$

Since we are in the matter era we set $\omega_m \equiv 0$.

Inserting eq.(1) into eq.(5) we can integrate the latter in order to obtain the Hubble parameter as a function of time:

$$H(t) = H_0 \sqrt{\frac{\Omega_\Lambda - \nu}{1 - \nu}} \coth \left[\frac{3}{2} H_0 \sqrt{(\Omega_\Lambda - \nu)(1 - \nu)} t \right]. \quad (6)$$

where $\Omega_\Lambda = 1 - \Omega_m$ and H_0 is the Hubble constant^a. Using $H = \dot{a}/a$ the cosmic time, $t(a)$, is given by

$$t(a) = \frac{2}{3\tilde{\Omega}_\Lambda^{1/2}(1 - \nu)H_0} \sinh^{-1} \left(\sqrt{\frac{\tilde{\Omega}_\Lambda}{\tilde{\Omega}_m}} a^{3(1-\nu)/2} \right) \quad (7)$$

where we have introduced

$$\tilde{\Omega}_m = \frac{\Omega_m}{1 - \nu}, \quad \tilde{\Omega}_\Lambda = \frac{\Omega_\Lambda - \nu}{1 - \nu}. \quad (8)$$

Inverting eq.(7) we easily determine the scale factor $a = a(t)$. Substituting the cosmic time into (6), one can provide the normalized Hubble parameter

$$E^2(a) = \frac{H^2(a)}{H_0^2} = \tilde{\Omega}_\Lambda + \tilde{\Omega}_m a^{-3(1-\nu)} \quad (9)$$

where the cosmological parameters obey the standard cosmic sum rule, namely $\tilde{\Omega}_m + \tilde{\Omega}_\Lambda = 1 = \Omega_m + \Omega_\Lambda$.

^aFor the comoving distance and for the dark matter halo mass (see section 4) we use the traditional parametrization $H_0 = 100h\text{km/s/Mpc}$. Of course, when we treat the power spectrum shape parameter Γ we utilize $h \equiv h_{\text{Planck}} = 0.673$ [2].

4 *Spyros Basilakos*

Concerning the evolution of matter density the situation is as follows. Combining eq.(1), (2) and (4) we arrive at $\dot{\rho}_m + 3H\rho_m = 3\nu H\rho_m$. Integrating the latter (using $\dot{\rho}_m = aHd\rho_m/da$) we find

$$\rho_m(a) = \rho_{m0} a^{-3(1-\nu)}, \quad (10)$$

where ρ_{m0} is the matter density at the present time ($a = 1$), and therefore $\Omega_m = \rho_{m0}/\rho_{c0}$, where $\rho_{c0} = 3H_0^2/8\pi G$ is the current critical density. In fact, defining $\Omega_m(a) \equiv \rho_m(a)/\rho_c(a)$ it is easy to see, with the help of (10) and the definition of $E(a)$, that

$$\Omega_m(a) = \frac{\Omega_m a^{-3(1-\nu)}}{E^2(a)}. \quad (11)$$

Lastly, upon inserting (10) in (4) and integrating once more in the scale factor variable, we arrive at the explicit expression for the evolution of the vacuum energy density:

$$\Lambda(a) = \Lambda_0 + 8\pi G \frac{\nu \rho_{m0}}{1-\nu} \left[a^{-3(1-\nu)} - 1 \right]. \quad (12)$$

Obviously, for $\nu = 0$ the current time varying vacuum model reduces to the concordance Λ cosmology as it should.

Using the above normalized Hubble parameter [see eq.(9)], a joint statistical analysis, involving the latest cosmological data [SNIa,¹⁵ $A(z)$ of BAOs¹⁶ and *Planck* CMB shift parameter^{2,18}] is implemented. Since the explored cosmological models (Λ_{RG} and Λ CDM) contain different number of free parameters, as a further statistical test we use the (*corrected*) Akaike Information Criterion (AIC) relevant to our case ($N_{\text{tot}}/k > 40$),¹⁹ which is given, in the case of Gaussian errors, as follows: $\text{AIC} = \chi_{\text{t,min}}^2 + 2k$, where $\chi_{\text{t}}^2 = \chi_{\text{SNIa}}^2 + \chi_{\text{BAO}}^2 + \chi_{\text{CMB}}^2$ is the overall χ^2 -function and k is the number of free parameters. From the statistical viewpoint, a smaller value of AIC points to a better model-data fit. Within this framework, we need to make clear that small differences in AIC are not necessarily significant and therefore, it is important to derive the model pair difference, namely $\Delta\text{AIC} = \text{AIC}_y - \text{AIC}_x$. The larger the value of $|\Delta\text{AIC}|$, the higher the evidence against the model with larger value of AIC, with a difference $|\Delta\text{AIC}| \geq 2$ indicating a positive such evidence and $|\Delta\text{AIC}| \geq 6$ indicating a strong such evidence, while a value ≤ 2 indicates consistency among the two comparison models. For the concordance Λ CDM cosmology, if we impose $\nu = 0$ and minimizing with respect to Ω_m we find $\Omega_m = 0.291 \pm 0.011$ with $\chi_{\text{t,min}}^2(\Omega_m)/dof \simeq 567.5/586$ ($\text{AIC}_\Lambda \simeq 569.5$). For comparison, we provide the results of *Planck*: $\Omega_m h^2 = 0.1426 \pm 0.0025$, with $h_{\text{Planck}} = 0.673 \pm 0.012$ which implies $\Omega_m = 0.315 \pm 0.016$. Notice that throughout the paper we set $\Omega_{m,\Lambda} \equiv \Omega_m = 0.291$. In the case of the Λ_{RG} model we find that the overall likelihood function peaks at $\Omega_m = 0.282 \pm 0.012$ and $\nu = 0.0048 \pm 0.0032$ with $\chi_{\text{t,min}}^2(\Omega_m, \nu) \simeq 563.8$ ($\text{AIC}_{\text{RG}} \simeq 567.8$) for 585 degrees of freedom.¹³ It turns out that the current vacuum model appears to fit slightly better than the Λ CDM

the observational data. Still, the $|\Delta\text{AIC}|=|\text{AIC}_\Lambda - \text{AIC}_{RG}|$ values (ie., ≤ 2) indicate that the cosmological data are simultaneously consistent with the cosmological models. Note that for the rest of the paper we will restrict our present analysis to the choice of $(\Omega_m, \nu) = (0.282, 0.0048)$.

Table 1. Statistical results from fitting SNIa+BAO+CMB_{shift} data. The 1st column indicates the model. The 2nd and 3rd columns provide the best fit parameters (Ω_m, ν) . The 4th and 5th columns list the statistical significance of the fit. Finally, the 6th and 7th columns shows the estimated values of (σ_8, δ_c) . Notice that in section 4 we provide a relevant discussion regarding δ_c .

Model	Ω_m	ν	$\chi_{t,\min}^2$	AIC	σ_8	δ_c
ΛCDM	0.291 ± 0.011	0	567.5	569.5	0.829	1.675
Λ_{RG}	0.282 ± 0.012	0.0048 ± 0.0032	563.8	567.8	0.758	1.644

3. CDM Power Spectrum - growth factor

The CDM power spectrum is given by $P(k) = P_0 k^n T^2(k)$, where $T(k)$ is the CDM transfer function and $n \simeq 0.9603$ following the recent analysis of the Planck data.² Concerning the form of $T(k)$, we use that of Eisenstein & Hu²⁰ $T(k) = \frac{L_0}{L_0 + C_0 q^2}$, where $q \equiv \frac{k}{\Gamma}$, $L_0 = \ln(2e + 1.8q)$, $e = 2.718$ and $C_0 = 14.2 + \frac{731}{1+62.5q}$. Here Γ is the shape parameter¹⁷ which is written as: $\Gamma = \Omega_m h_{\text{Planck}} \exp(-\Omega_b - \sqrt{2h_{\text{Planck}}} \Omega_b / \Omega_m)$. The value of Γ , which is kept constant throughout the model fitting procedure, is estimated using the *Planck* results $\Omega_b = 0.0222 h_{\text{Planck}}^{-2}$ with $h_{\text{Planck}} = 0.672$.

Another important quantity here is the rms fluctuations of the linear density field on mass scale M_h :

$$\sigma^2(M, z) = \sigma_8^2(z) \frac{\int_0^\infty k^{n_s+2} T^2(\Omega_m, k) W^2(kR) dk}{\int_0^\infty k^{n_s+2} T^2(\Omega_m, k) W^2(kR_8) dk}, \quad \sigma_8(z) = \sigma_8 \frac{D(z)}{D(0)}. \quad (13)$$

where $\sigma_8 \equiv \sigma(R_8, 0)$ is the rms mass fluctuation on $R_8 = 8h^{-1}$ Mpc scales. At this point we would like to remind the reader that $D(z)$ is the growth factor (see below), $W(kR) = 3(\sin kR - kR \cos kR)/(kR)^3$ and $R = (3M_h/4\pi\rho_{m0})^{1/3}$ with $\rho_{m0} = \Omega_m \rho_{c0}$ denotes the mean matter density of the universe at the present time ($\rho_{m0} = 2.78 \times 10^{11} \Omega_m h^2 M_\odot \text{Mpc}^{-3}$). In this work we use the *Planck* prior, namely $\sigma_{8,\Lambda} = 0.829$. Of course, in order to use σ_8 properly along the current vacuum model we need to rescale the value of σ_8 by

$$\sigma_8 = \sigma_{8,\Lambda} \frac{D(0)}{D_\Lambda(0)} \left[\frac{P_0 \int_0^\infty k^{n_s+2} T^2(\Omega_m, k) W^2(kR_8) dk}{P_{0,\Lambda} \int_0^\infty k^{n_s+2} T^2(\Omega_{m,\Lambda}, k) W^2(kR_8) dk} \right]^{1/2}, \quad (14)$$

where $P_0/P_{0,\Lambda} = (\Omega_{m,\Lambda}/\Omega_m)^2$. Based on the aforementioned observational constraints and eq.(14) we find $\sigma_8 = 0.758$ for the Λ_{RG} model. In Table 1, one may see a more compact presentation of the cosmological parameters including the δ_c which

6 *Spyros Basilakos*

is the linearly extrapolated density threshold above which structures collapse (see section 4).

Now we focus on the basic equation which describes the evolution of matter fluctuations within the context of the previously described vacuum model. At sub-horizon scales the corresponding time evolution equation (in the linear regime) for the matter density contrast $D \equiv \delta\rho_m/\rho_m$, in a pressureless fluid, is given by (see Refs. [8, 21]):

$$\ddot{D} + (2H + Q)\dot{D} - (4\pi G\rho_m - 2HQ - \dot{Q})D = 0, \quad (15)$$

where in our case $Q(t) = -\dot{\Lambda}/\rho_m$. It becomes clear, that the interacting vacuum energy affects the growth factor via the function $Q(t)$. In the case of non interacting DE models, [$Q(t) = 0$], the above equation (15) reduces to the usual time evolution equation for the mass density contrast.^{22,23} For the concordance Λ cosmology it is easy to prove that the solution of eq.(15) is²²

$$D_\Lambda(a) = \frac{5\Omega_m E(a)}{2} \int_0^a \frac{dx}{x^3 E^3(x)}. \quad (16)$$

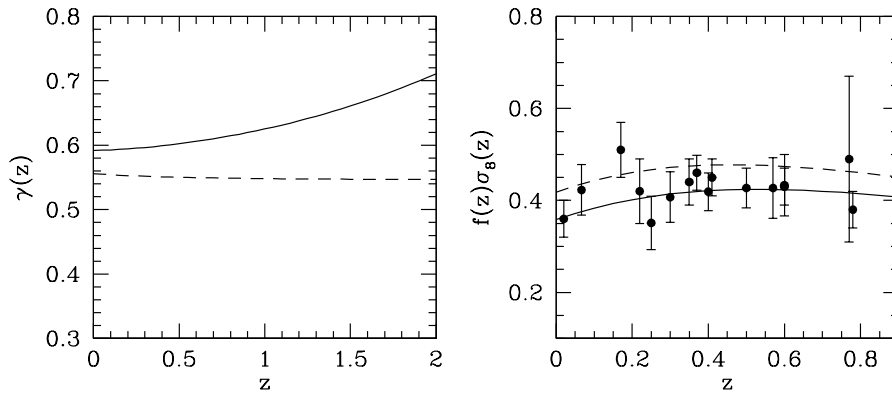


Fig. 1. *Right Panel:* Comparison of the observed and theoretical evolution of the growth rate $f(z)\sigma_8(z)$. The dashed line corresponds to the Λ CDM ($\sigma_{8,\Lambda} = 0.829$) and the solid one is for Λ_{RG} ($\sigma_8 = 0.758$). *Left Panel:* The evolution of the growth index of matter perturbations.

For the purpose of our study it is important to solve eq.(15) in order to investigate the matter fluctuation field of the vacuum model (1) in the linear regime. Here we present the main steps (for more details see Ref. [11]). First of all we change variables from t to a new one according to the transformation

$$y = \coth \left[\frac{3}{2} H_0 \sqrt{(\Omega_\Lambda - \nu)(1 - \nu)} t \right]. \quad (17)$$

Also from equations (6), (7) and (9) we get the following useful relations:

$$y = \sqrt{\frac{1 - \nu}{\Omega_\Lambda - \nu}} E(a), \quad y^2 - 1 = \frac{\Omega_m}{\Omega_\Lambda - \nu} a^{-3(1-\nu)}. \quad (18)$$

Utilizing (17) and (18) we find, after some non-trivial algebra, that equation (15) becomes

$$3\beta^2(y^2 - 1)^2 D'' + k(\beta)y(y^2 - 1)D' - 2[g(\beta)y^2 - \psi(\beta)]D = 0, \quad (19)$$

a solution of which is

$$D(y) = C(y^2 - 1)^{\frac{4-9\beta}{6\beta}} y F\left(\frac{1}{3\beta} + \frac{1}{2}, \frac{3}{2}, \frac{1}{3\beta} + \frac{3}{2}, -\frac{1}{y^2 - 1}\right) \quad (20)$$

where $\beta \equiv 1 - \nu$, primes denote derivatives with respect to y , the quantity F is the hypergeometric function, $k(\beta) = 2\beta(6\beta - 5)$, $g(\beta) = (2 - \beta)(3\beta - 2)$ and $\psi(\beta) = \beta(4 - 3\beta)$. Now inserting eq.(18) into eq.(20) and using eq.(8), we finally obtain the growth factor $D(a)$ as a function of the scale factor:

$$D(a) = C_1 a^{\frac{9\beta-4}{2}} E(a) F\left(\frac{1}{3\beta} + \frac{1}{2}, \frac{3}{2}, \frac{1}{3\beta} + \frac{3}{2}, -\frac{\tilde{\Omega}_\Lambda}{\tilde{\Omega}_m} a^{3\beta}\right) \quad (21)$$

where $C_1 \propto C$ is an integration constant to be adjusted by an initial condition.^b

Furthermore, a crucial role in structure formation studies plays the growth rate of clustering which is defined as $f(a) = \frac{d \ln D}{d \ln a} \simeq \Omega_m^\gamma(a)$ where γ is the growth index. It has been shown that for those dark energy models which have a slow varying equation of state parameter, the growth index γ is well approximated by $\gamma \simeq \frac{3(w-1)}{6w-5}$ (see Refs. [24, 25, 26]), or $\gamma \simeq 6/11$ in the case where $w = -1$ (Λ CDM model). Now since we know the analytical form of the growth factor $D(a)$ one may directly compute the evolution of $f(a)$.

In order to test the performance of the Λ_{RG} vacuum model at the perturbation level, we utilize the recent growth rate data for which their combination parameter of the growth rate of structure, $f(z)$, and the redshift-dependent rms fluctuations of the linear density field, $\sigma_8(z)$, is available as a function of redshift, $f(z)\sigma_8(z)$. The total sample contains $N = 16$ entries (as collected by Ref. [27] - see their Table 1 and references therein). In the right panel of figure 1 we present the growth data (solid points) together with the predicted $f(z)\sigma_8(z)$ for the running vacuum model (solid line) and Λ CDM (dashed line). We find that the concordance Λ cosmology (with $\Omega_m = 0.291$) reproduce the growth data with $\chi_{\min}^2/dof \simeq 20.02/15$ implying that the Λ CDM model can not simultaneously accommodate the *Planck* priors and the growth data (see also Ref. [28]). On the other hand for the Λ_{RG} model we have $\chi_{\min}^2/dof \simeq 8.42/15$. Performing the AIC information criterion for small sample size, namely $AIC = \chi_{\min}^2 + 2k + \frac{2k(k-1)}{N-k-1}$ we find $\Delta AIC = AIC_\Lambda - AIC_{RG} \simeq 11.6$ which means that the growth data favor the current running vacuum scenario.

Let us finish this section with a relevant discussion regarding the growth index γ . As we have already described, we can express the linear growth rate of clustering in terms of the growth index. Specifically, from $\frac{d \ln D}{d \ln a} \simeq \Omega_m^\gamma(a)$ we easily obtain: $\gamma(z) \simeq \frac{\ln[-(1+z) \frac{d \ln D}{dz}]}{\ln \Omega_m(z)}$, where $z = a^{-1}(z) - 1$. Based on the aforesaid observational

^bWe normalize the growth factor at large redshifts ($z \gg 1$), namely $D(z) \simeq 1/(1+z)$.

constraints we find that the growth index at the present time becomes $\gamma_{\Lambda_{RG}} \simeq 0.58$ which is somewhat higher with respect to the Λ CDM value, namely $\gamma \simeq 6/11$. In the left panel of figure 1 we show the growth index evolution for the Λ_{RG} and Λ CDM models, respectively. From the comparison we observe that the growth index of the Λ_{RG} vacuum model deviates from the concordance model. In particular, there is a visible deviation from above in all the redshift range. This deviation becomes at the level of 10% for $z \leq 1$.

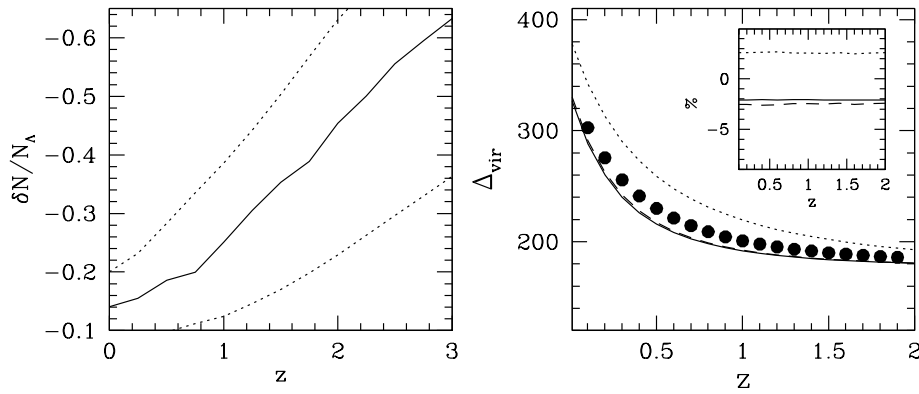


Fig. 2. *Left Panel:* Fractional difference $\delta N / N_\Lambda$ (solid line) in the cluster number counts between the Λ_{RG} model and the reference Λ CDM model. The dotted curves correspond to 2σ Poisson uncertainties. Notice that we use the priors of Table 1. *Right Panel:* In the inner panel we provide the relative deviation $(1 - \lambda/\lambda_\Lambda)\%$ of the collapse factor for various vacuum models with respect to the Λ solution. In the outer panel we observe the evolution of the virial density. The lines corresponds to the following vacuum models: (i) Λ_{RGH} (solid), (ii) Λ_{RGC1} (dashed line, $\nu_s = 0.002$) and (iii) Λ_{RGC2} (dotted line, $\nu_s = -0.002$). Notice that the solid points represent the concordance Λ CDM cosmology.

4. Comparison with Cluster Halo Abundances

Another choice in order to discriminate the models, that has been extensively used so far in the literature, is to estimate the theoretical predictions of the models for the cluster-size halo redshift distributions and to confront them with the data. The halo abundances predicted by a large variety of time varying vacuum models have been compared with those corresponding to the Λ CDM model.^{11–13, 29} We utilize the Press and Schechter³⁰ formalism, which determines the fraction of matter that has formed bounded structures as a function of redshift. Mathematical details of such a treatment can be found also in Ref. [13]; here we only present the basic ideas. The number density of halos, $n(M, z)$, with masses within the range $(M, M + \delta M)$ is given by:

$$n(M, z)dM = \frac{\bar{\rho}}{M} \frac{d \ln \sigma^{-1}}{dM} f(\sigma) dM, \quad (22)$$

where $\bar{\rho} = \rho_{m0}$ is the mean background mass density (see section 3). In the original Press-Schechter (PSc) formalism, $f(\sigma) = f_{\text{PSc}}(\sigma) = \sqrt{2/\pi}(\delta_c/\sigma) \exp(-\delta_c^2/2\sigma^2)$, δ_c is the linearly extrapolated density threshold above which structures collapse,³¹ while $\sigma^2(M, z)$ is the mass variance of the smoothed linear density field, extrapolated to redshift z at which the halos are identified [see eq.(13)]. The mass variance depends on the power-spectrum of density perturbations in Fourier space, $P(k)$, for which we use here the CDM form according to Ref. [20], and the values of the baryon density parameter, the spectral slope and Hubble constant according to the recent *Planck* results.² Although the original Press-Schechter mass-function, f_{PSc} , was shown to provide a good first approximation to that provided by numerical simulations, it was later found to over-predict/under-predict the number of low/high mass halos at the present epoch.^{32,33} More recently, a large number of works have provided better fitting functions of $f(\sigma)$, some of them based on a phenomenological approach. In the present study, we adopt the one proposed by Reed *et al.* [34].

In order to compare the mass function predictions of the different cosmological models, it is important to use for each model the corresponding value of σ_8 and δ_c (see Table 1). It is well known that for the usual Λ cosmology we have $\delta_c \simeq 1.675$ (see Ref.[35]). For the Λ_{RG} model it has been found that $\delta_c \simeq 1.644$ (see Ref. [13]). Given the halo mass function from eq.(22) we can now derive an observable quantity which is the redshift distribution of clusters, $\mathcal{N}(z)$, within some determined mass range, say $M_1 \leq M/h^{-1}M_\odot \leq M_2 = 10^{16}$. This can be estimated by integrating over mass the expected differential halo mass function, $n(M, z)$:

$$\mathcal{N}(z) = \frac{dV}{dz} \int_{M_1}^{M_2} n(M, z) dM, \quad \frac{dV}{dz} = \Omega_s r^2(z) \frac{dr}{dz}, \quad r(z) = c \int_0^z \frac{du}{H(u)}, \quad (23)$$

where dV/dz is the comoving volume element and Ω_s is the solid angle.

In left panel of figure 2, we present the fractional difference between the Λ_{RG} model and Λ CDM namely, $\delta\mathcal{N}/\mathcal{N}_\Lambda$, with masses in the range $10^{13.4} h^{-1} \lesssim M/M_\odot \lesssim 10^{16} h^{-1}$. Recall that we denote the deviations of the number counts of a given vacuum model with respect to the Λ CDM as $\delta\mathcal{N} = \mathcal{N} - \mathcal{N}_\Lambda$. The dotted lines shown in the left panel of figure 2 correspond to 2σ Poisson uncertainties, which however do not include cosmic variance and possible observational systematic uncertainties, that would further increase the relevant variance. Specifically, the prediction for $\delta\mathcal{N}/\mathcal{N}$ is negative for all points, even for those in the $\pm 1\sigma$ band. Thus, the running vacuum model tends to predict a smaller number of counts as compared to the Λ CDM. The fractional decrease can be as significant as 30 – 60%. We also find that the redshift variation of the differences between the Λ_{RG} cosmology and Λ CDM model is mainly affected by variations in the values of σ_8 and δ_c (for more discussion see Ref. [13]). Therefore, we have verified that there are observational signatures that can be used to differentiate the Λ_{RG} model from the Λ CDM and possibly from a large class of DE models.

5. The spherical collapse model

In this section we generalize the spherical collapse model within the variable $\Lambda(H)$ cosmological model, in order to understand non-linear structure formation in such scenarios and investigate the differences with the corresponding expectations of the concordance Λ CDM cosmology. Practically, one may start from the Raychaudhuri equation which is valid either for the entire universe or for homogeneous spherical perturbations [by replacing the scale factor with radius $R(t)$]

$$\frac{\ddot{R}}{R} = -\frac{4\pi G}{3} (\rho_{ms} - 2\rho_{\Lambda s}), \quad (24)$$

where ρ_{ms} and $\rho_{\Lambda s}$ refer to the corresponding values of the matter and vacuum energy densities in the spherical patch susceptible of ulterior collapse.

Now let us first define some basic quantities of the problem. In particular, we call α_t the scale factor of the universe where the overdensity reaches at its maximum expansion (i.e. when $\dot{R} = 0$) and α_c the scale factor in which the sphere virializes, implying that a cosmic structure has formed. Also, R_t and R_c denote the corresponding radii of the spherical overdensity, the former being the turnaround (or “top hat”) value at the point of maximum size, and the latter refers to the eventual situation when the sphere has already collapsed and virialized. We would like to remind the reader that due to the coupling between the running vacuum and matter one would expect that the matter density in the spherical overdensity should obey the same power law as the background matter $\rho_m(a) \propto a^{-3(1-\nu)}$ (see eq.10). Thus, $\rho_{ms} \propto R^{-3(1-\nu)}$ denotes the matter density in the spherical patch. Regarding, the vacuum energy density in the spherical region, $\rho_{\Lambda s}$ we focus on two situations: (i) the vacuum energy remains homogeneous and only the corresponding matter virializes (this scenario holds for the Λ cosmology); and (ii) the case with clustered vacuum energy, assuming that the whole system virializes (both matter and vacuum components).

In the regime where the vacuum is allowed to cluster we have $\rho_{\Lambda s}(R) = \Lambda_s(R)/8\pi G$. Therefore, in such a situation it could be possible, on non-linear scales, to have an interaction between dark matter and dark energy with a different ν than the background value. We also assume that the general functional form that describes the behavior of the vacuum energy density inside the spherical perturbation obeys a similar equation as that of eq.(12):

$$\Lambda_s(R) = \Lambda_0 + 8\pi G \frac{\nu_s \rho_{ms,t}}{1 - \nu_s} \left[\left(\frac{R}{R_t} \right)^{-3(1-\nu_s)} - 1 \right]. \quad (25)$$

where ν_s is not necessarily equal to the background ν .

Using the basic differential equations [see eq.(2) and (24)] and performing the following transformations $x = a/a_t$ and $y = R/R_t$ we arrive at

$$\dot{x}^2 = H_t^2 \Omega_{m,t} [x^{-1+3\nu} + r x^2 I(x)] \quad (26)$$

and

$$\frac{\ddot{y}}{y} = -\frac{H_t^2 \Omega_{m,t}}{2} \left[\frac{\zeta}{y^{3(1-\nu)}} - 2 \frac{\rho_{\Lambda s}}{\rho_{m,t}} \right]. \quad (27)$$

where $H_t^2 \Omega_{m,t} = \frac{8\pi G}{3} \rho_{m,t}$. Notice that $\Omega_{m,t} \equiv \Omega_m(a_t)$ is the matter density parameter at the turnaround epoch (see eq.11).

It is important to point that in order to obtain the above set of equations we have used the following relations:

$$\rho_{ms} = \rho_{ms,t} \left(\frac{R}{R_t} \right)^{-3(1-\nu)} = \frac{\zeta \rho_{m,t}}{y^{3(1-\nu)}}, \quad (28)$$

$$I(x) = \frac{\rho_{\Lambda}}{\rho_{\Lambda,t}} = \frac{1 + \nu \tilde{r}_0 a_t^{-3(1-\nu)} x^{-3(1-\nu)}}{1 + \nu \tilde{r}_0 a_t^{-3(1-\nu)}}, \quad (29)$$

and

$$r = \frac{\rho_{\Lambda,t}}{\rho_{m,t}} = \frac{\Omega_{\Lambda}}{\Omega_m} a_t^{3(1-\nu)} + \frac{\nu}{1-\nu} \left[1 - a_t^{3(1-\nu)} \right] \quad (30)$$

where $\tilde{r}_0 = \tilde{\Omega}_{\Lambda}/\tilde{\Omega}_m$, $\rho_{m,t}$, $\rho_{\Lambda,t}$ are the matter and the vacuum energy density at the turnaround epoch which satisfies $\Omega_{\Lambda,t} = 1 - \Omega_{m,t}$ (for definition see eq.11). Of course we need to say that in order to derive eqs.(29) and (30) we have used eqs.(8) and (12). The matter density in the spherical region at the turn around time is given with respect to the background matter density at the same epoch $\rho_{m,t}$ as $\rho_{ms,t} = \zeta \rho_{m,t}$. The parameter ζ is the density contrast at the turnaround point. It is interesting to mention that in the case of the Einstein-de Sitter model ($\tilde{\Omega}_m = \Omega_m = 1$ and $\nu = 0$) the solution of the system formed by eq.(26) and eq.(27) reduces to the well known value of the density contrast at the turnaround point: $\zeta = \left(\frac{3\pi}{4}\right)^2$, as it should.

For bound perturbations which do not expand forever, the time needed to re-collapse is twice the turn-around time, $t_c \simeq 2t_t$. Therefore, from eq.(7), we obtain the relation between the α_c and α_t $\sinh^{-1} \left[\sqrt{\tilde{r}_0} a_c^{3(1-\nu)} \right] \simeq 2 \sinh^{-1} \left[\sqrt{\tilde{r}_0} a_t^{3(1-\nu)} \right]$ which is well approximated by $z_t \simeq 1.523z_c + 0.8$. Therefore, considering that clusters have virialized at the present epoch, $z_c \simeq 0$, the turnaround redshift is $z_t \simeq 0.8$. If we assume that galaxy clusters have formed close to the epoch of $z_c \sim 1.5$ then we obtain $z_t \sim 3$. To this end we verify that the ratio between the scale factors converges to the Einstein de Sitter value $(a_c/a_t)_{\Lambda_{RG}} \simeq (1+z_t)/(1+z_c) = 2^{2/3}$ at high redshifts owing to the fact that the matter component dominates the Hubble expansion.

In order to provide the virial theorem of the Λ_{RG} model we need to generalize the Layzer-Irvine equation, which describes the flow to virialization.²² If we take into account that the matter is exchanging energy with the vacuum then the modified virial theorem becomes³⁷

$$(2 - 3\nu)T + (1 - 6\nu)(U_G - 2U_{\Lambda}) = 0 \quad (31)$$

12 *Spyros Basilakos*

where $U_G = 3GM^2/5R$. The vacuum potential energy U_Λ is written as

$$U_\Lambda = \begin{cases} -\frac{\Lambda(a)MR^2}{10} & \text{Homogeneous} \\ -\frac{\Lambda_0 MR^2}{10} + \frac{4\pi G\nu_s M\rho_{m,s,t} R^{10}}{5(1-\nu_s)} - \frac{4\pi G\nu_s M\rho_{m,s,t} R^{-1+3\nu_s}}{(1-\nu_s)(2+3\nu_s)R_t^{-3(1-\nu)}} & \text{Clustered} \end{cases} \quad (32)$$

where M is the mass inside the spherical overdensity. Utilizing the observational constraint $\nu = 0.0048$, the deviation from the usual virial condition is $\sim 2 - 3\%$. In this context, combining the virial theorem and the energy conservation ($T_c + U_{G,c} + U_{\Lambda,c} = U_{G,t} + U_{\Lambda,t}$) at the collapse and at the turn around epochs we reach to the following condition:

$$q_1(\nu)U_{G,c} + q_2(\nu)U_{\Lambda,c} = U_{G,t} + U_{\Lambda,t}, \quad q_1(\nu) = \frac{1+3\nu}{2-3\nu}, \quad q_2(\nu) = \frac{4-15\nu}{2-3\nu}. \quad (33)$$

Clearly, for $\nu = 0$ the above equations boil down to those of the Λ model.

5.0.1. Homogeneous vacuum

In the case of homogeneous vacuum (hereafter Λ_{RGH}) model we have $\rho_{\Lambda s}(a) = \rho_\Lambda(a) = \Lambda(a)/8\pi G$. Within this framework, inserting eq.(29) into eq.(27), we obtain

$$\ddot{y} = -\frac{H_t^2 \Omega_{m,t}}{2} \left[\frac{\zeta}{y^{2-3\nu}} - 2ryI(x) \right]. \quad (34)$$

The solution for ζ is provided only numerically by integrating the main system of differential equations, (eqs.26 and 34), using the boundary conditions: $(dy/dx) = 0$ and $y = 1$ at $x = 1$. However, we find that a reasonably accurate fitting formula for ζ is given by

$$\zeta \simeq \left(\frac{3\pi}{4} \right)^2 \Omega_{m,t}^{-\omega_1 + \omega_2 \Omega_{m,t} - \omega_3 w(a_t)}, \quad (\omega_1, \omega_2, \omega_3) = (0.79, 0.26, 0.06) \quad (35)$$

where $w(a) = -1 - \frac{\nu a^{3\nu}}{a^{3\nu} + \bar{r}_0}$. Using eqs.(32),(33) and $U_G = 3GM^2/5R$ we can obtain a cubic equation that relates the ratio between the virial R_c and the turn-around outer radius R_t the so called collapse factor ($\lambda = R_c/R_t$), $q_2(\nu)n_c\lambda^3 - (2+n_t)\lambda + 2q_1(\nu) = 0$, where

$$n_{c,t} = \frac{\Lambda(a_{c,t})}{4\pi G\rho_{m,t}\zeta} = n_0 + \frac{2\nu a_t^{3(1-\nu)}}{\zeta(1-\nu)} \left[a_{c,t}^{-3(1-\nu)} - 1 \right] \quad (36)$$

with $n_0 = \frac{2\Omega_\Lambda a_t^{3(1-\nu)}}{\Omega_m \zeta}$. The viable solution ($0 < \lambda < 1$) of the above cubic equation is

$$\lambda = -\frac{2d^{1/3}}{3} \cos\left(\frac{\theta - 2\pi}{3}\right), \quad d = \sqrt{x_1^2 + x_2^2}, \quad \theta = \cos^{-1}(x_1/d) \quad (37)$$

where $x_1 = -27q_1$, $x_2 = -\frac{3\sqrt{3\mathcal{D}}}{2}$ and $\mathcal{D} = 4 \frac{(2+n_t)^3 - 27q_1^2 q_2 n_c}{q_2^3 n_c^3}$. Of course in the case of $\nu = 0$ the above expressions get the usual form for Λ cosmology^{38,39} while for an Einstein-de Sitter model ($\Omega_m = 1$) we have $\lambda = 1/2$.

We find that the collapse factor lies in the range $\lambda \simeq 0.48 - 0.50$ in agreement with previous studies.^{39–43,45,46} In the inner panel of figure 2 we plot the relative deviation (solid line) of the collapse factors $\lambda_{\Lambda_{RGH}}(z_c)$ for the current vacuum model with respect to the Λ solution $\lambda_{\Lambda}(z_c)$. Obviously, the deviation from the Λ CDM case is small $\sim -2\%$. In the outer panel of figure 2 we present the evolution of the density contrast at virialization (solid curve)

$$\Delta_{vir} = \frac{\rho_{ms,c}}{\rho_{m,c}} = \frac{\zeta}{\lambda^3} \left(\frac{a_c}{a_t} \right)^3. \quad (38)$$

We verify, that the density contrast decreases with the virialization redshift $z \equiv z_c$ and at very large redshifts it tends to the Einstein-de Sitter value ($\Delta_{vir} \sim 18\pi^2$), since the matter component dominates the cosmic fluid. Following the notations of Ref. [35], we obtain an accurate fitting formula to Δ_{vir} (within a physical range of cosmological parameters and for $z < 2$)

$$\Delta_{vir}(a) \simeq 18\pi^2 [1 + \epsilon \Theta^b(a)], \quad \Theta(a) = \Omega_m^{-1}(a) - 1, \quad (39)$$

where $\epsilon = 0.40 - 23.2\nu + 500\nu^2$ and $b = 0.94 + 39.6\nu$. From the right panel of figure 2 we observe that the virial density Δ_{vir} of the Λ_{RGH} model is somewhat lower with respect to that of Λ CDM model, namely the relative difference can reach up to $\sim -4\%$. As an example, assuming that clusters have formed prior to the epoch of $z_c \simeq 1.5$ ($z_t \sim 3$) we find $(\zeta, \Delta_{vir})_{\Lambda_{RGH}} \simeq (5.66, 183.9)$ and $(\zeta, \Delta_{vir})_{\Lambda} \simeq (5.65, 190)$. To conclude this discussion we would like to stress that in the homogeneous case the dark energy (in our case vacuum) component flows progressively out of the overdensity^{41,44} and hence energy conservation cannot be applied. Such violation is however only important for large values of $|\nu| \simeq \mathcal{O}(10^{-2})$ and at very late times, when the vacuum energy dominates the cosmic fluid.

5.0.2. Clustered vacuum

In this section we assume that the vacuum clusters along with the dark matter. As we have already mentioned the vacuum inside the spherical patch is given by eq.(25). In the current study we restrict our analysis to $\nu_s = 0.002$ (hereafter Λ_{RGC1} : dashed line) and $\nu_s = -0.002$ (hereafter Λ_{RGC2} : dotted line). Substituting $y = R/R_t$ into eq.(25) we have

$$\Lambda_s(y) = \Lambda_0 + 8\pi G \frac{\nu_s \zeta \rho_{m,t}}{1 - \nu_s} \left[y^{-3(1-\nu_s)} - 1 \right], \quad (40)$$

where the vacuum energy density is $\rho_{\Lambda_s}(y) = \Lambda_s(y)/8\pi G$. The merit of the latter assumption is that it allows an analytical solution to the system of eqs.(26) and (27). Indeed inserting the above form of $\rho_{\Lambda_s}(y)$ into eq (27) we obtain

$$\ddot{y} = -\frac{H_t^2 \Omega_{m,t}}{2} \left[\frac{(1 - 3\nu_s)\zeta}{(1 - \nu_s)y^{2-3\nu_s}} - 2 \left(r - \frac{\nu_s \zeta}{1 - \nu_s} \right) y \right]. \quad (41)$$

14 *Spyros Basilakos*

and upon integration we find

$$\dot{y}^2 = H_t^2 \Omega_{m,t} [P(y, \zeta) + C], \quad (42)$$

where C is the integration constant and $P(y, \zeta) = \frac{\zeta}{(1-\nu_s)y^{1-3\nu_s}} + \left(r - \frac{\nu_s \zeta}{1-\nu_s}\right) y^2$. Notice that the boundary conditions, $(dy/dx) = 0$ and $y = 1$ at $x = 1$, imply that $C = -P(1, \zeta)$. Combining eq.(42) with the background equation (26) the solution of the system is

$$\int_0^1 \frac{dy}{\sqrt{P(y, \zeta) - P(1, \zeta)}} = \int_0^1 \frac{dx}{\sqrt{x^{-1+3\nu} + rx^2 I(x)}}. \quad (43)$$

Furthermore, if the vacuum energy participates in the virialization then the potential energy of the vacuum is given by the second branch of eq.(32). In this case, using simultaneously eqs.(32),(33) and $U_G = 3GM^2/5R$ the collapse factor obeys

$$q_2(\nu_s)[n_0 - f(\nu_s)]\lambda^3 - A(n_0, \nu_s)\lambda + g(\nu_s)\lambda^{3\nu_s} + 2q_1(\nu_s) = 0, \quad (44)$$

where

$$f(\nu_s) = \frac{2\nu_s}{1-\nu_s}, \quad g(\nu_s) = \frac{10\nu_s q_2(\nu_s)}{(1-\nu_s)(2-3\nu_s)}, \quad A(n_0, \nu_s) = 2 + n_0 - f(\nu_s) + \frac{g(\nu_s)}{q_2(\nu_s)}.$$

Finally, solving eqs.(43) and (44), we can estimate the density contrast at virialization from eq.(38). Similarly, as in section 6.2.1, the fitting formulas for ζ as well as for Δ_{vir} are given by eq.(35) and eq.(39). The corresponding parameters of the approximated formulas are

$$(\omega_1, \omega_2, \omega_3) = \begin{cases} (0.62, -0.08, 0.06) & 0 \leq \nu_s \leq 0.003 \\ (0.82, 0.22, 0.06) & -0.003 \leq \nu_s < 0 \end{cases} \quad (45)$$

$$(b, \epsilon) = \begin{cases} (0.94 + 90\nu_s, 0.40 - 46\nu_s + 500\nu_s^2) & -0.002 < \nu_s \leq 0.003 \\ (0.94 + 95\nu_s, 0.31 - 129\nu_s + 500\nu_s^2) & -0.003 \leq \nu_s \leq -0.002 \end{cases} \quad (46)$$

In this framework the collapse factor obeys $0.46 \leq \lambda \leq 0.52$. Also from figure 2 (see inner and outer panels) we see that the largest positive deviation of the collapse factor occurs for the Λ_{RGC2} model (dotted line). This implies that Λ_{RGC2} model forms more bound systems than the concordance Λ CDM model (solid points) and thus the corresponding cosmic structures should be located in larger density environments. Indeed, at the cluster formation epoch $z_c \simeq 1.5$ we obtain $(\zeta, \Delta_{vir})_{\Lambda_{RGC2}} \simeq (5.66, 202)$. The opposite situation holds for the Λ_{RGC1} model. From figure 2 it becomes obvious that the size and Δ_{vir} of the cosmic structures which are produced in the Λ_{RGC1} model (dashed line) are remarkably close to that predicted by the Λ_{RGH} vacuum cosmology, and therefore the impact of the vacuum energy on the spherical collapse is very small in the clustered case as long as ν_s is positive. In other words we find that both Λ_{RGH} and Λ_{RGC1} models are equivalent at the background and perturbation levels. Finally, at the epoch of $z_c \simeq 1.5$ we find $(\zeta, \Delta_{vir})_{\Lambda_{RGC1}} \simeq (5.70, 184.2)$. For comparison we provide the density pair of the Λ_{RGH} model, namely $(\zeta, \Delta_{vir})_{\Lambda_{RGH}} \simeq (5.66, 183.9)$.

6. Conclusions

In this review article we have studied the overall dynamics of the FLRW flat cosmological models in which the vacuum energy varies with the Hubble parameter, namely $\Lambda(H) = \Lambda_0 + 3\nu(H^2 - H_0^2)$. First we have performed a joint likelihood analysis in order to put constraints on the main cosmological parameters by using the current observational data (SNIa, BAOs and CMB shift parameter together with the growth rate of galaxy clustering). We have shown that the $\Lambda(H)$ model fits slightly better the observational data than that of the traditional Λ cosmology. In particular, we have found that the Λ CDM model can not simultaneously accommodate the *Planck* priors and the growth data implying that this kind of data favor the $\Lambda(H)$ vacuum scenario. Subsequently we have investigated the nonlinear regime and considered the predicted redshift distribution of cluster-size collapsed structures as a powerful method to distinguish the $\Lambda(H)$ and Λ CDM cosmological scenarios. Finally, we have generalized the properties (virial theorem, collapse factor, virial and turnaround densities) of the spherical collapse model in the case when the vacuum energy is a running function of the Hubble rate, $\Lambda = \Lambda(H)$. Overall, we have found that the virial density contrast is affected by the considered status of the vacuum energy model (homogeneous or clustered).

Acknowledgments: I would like to thank J. Solà, M. Plionis, J. A. S. Lima D. Polarski, N. E. Mavromatos, L. Perivolaropoulos and A. Gomez-Valent for the recent collaboration in some of the work presented in this review article.

References

1. M. Hicken et al., *Astrophys. J.*, **700**, 1097 (2009)
2. Planck Collaboration (P.A.R. Ade et al.), *Astron. Astrophys.* **in press** (2014) [arXiv:1303.5076]
3. S. Weinberg, *Rev. Mod. Phys.*, **61**, 1 (1989)
4. P. J. Steinhardt, in: *Critical Problems in Physics*, edited by V.L. Fitch, D.R. Marlow and M.A.E. Dementi (Princeton Univ. Pr., Princeton, 1997)
5. L. Amendola and S. Tsujikawa, *Dark Energy: Theory and Observations*, Cambridge University Press, Cambridge UK (2010)
6. O. Bertolami, *Nuovo Cimento B* **93**, 36 (1986); K. Freese et al. *Nuclear Physics B* **287**, 797 (1987); I. Waga, *Astrophys. J.* **414**, 436 (1993); J. A. S. Lima and J. M. F. Maia, *Phys. Rev. D* **49**, 5597 (1994); J. M. Overduin and S. Cooperstock, *Phys. Rev. D* **58**, 043506 (1998)
7. J. C. Carvalho, J. A. S. Lima and I. Waga, *Phys. Rev. D.*, **46**, 2404 (1992)
8. R. C. Arcuri and I. Waga., *Phys. Rev. D.*, **50**, 2928 (1994)
9. I. L. Shapiro and J. Solà, *Phys. Lett. B.*, **475**, 236, (2000); *JHEP* **0202**, 006, (2002); A. Babić, B. Guberina, R. Horvat and H. Štefančić, *Phys. Rev.* **D65**, 085002, (2002); *Phys. Rev.* **D71**, 124041, (2005)
10. I.L. Shapiro, J. Solà, C. España-Bonet and P. Ruiz-Lapuente, *Phys. Lett.* **B574**, 149, (2003); *JCAP* **0402**, 006, (2004); I.L. Shapiro and J. Solà, *Nucl. Phys. Proc. Supp.* **127**, 71, (2004); J. Solà, *J. of Phys.* **A41**, 164066, (2008); I.L. Shapiro and J. Solà, *Phys. Lett. B.*, **682**, 8 (2009)
11. S. Basilakos, M. Plionis and J. Solà, *Phys. Rev.* **D80**, 3511 (2009)

12. J. Grande, J. Solà, S. Basilakos and M. Plonis, JCAP **08**, 007 (2011); S. Basilakos, D. Polarski and J. Solà, Phys. Rev. D., **86**, 043010 (2012); E. L. D. Perico, J. A. S. Lima, S. Basilakos and J. Solà, Phys. Rev. D., **88**, 063531 (2013); J. A. S. Lima, S. Basilakos, and J. Solà, Mon. Not. R. Astron. Soc. **431**, 923 (2013)
13. A. Gómez-Valent, J., Solà, S. Basilakos, JCAP **in press**, (2015) [arXiv:1409.7048]
14. P. Wang and X.-H. Meng, Class. Quant. Grav. **22**, 283 (2005); J. S. Alcaniz and J. A. S. Lima, Phys. Rev. D. **72**, 063516 (2005); J. D. Barrow and T. Clifton, Phys. Rev. D., **73**, 103520 (2006); A. E. Montenegro and S. Carneiro, Class. Quant. Grav. **24**, 313 (2007); F. Bauer, Class. Quant. Grav., **22**, 3533 (2005); S. Carneiro and R. Tavakol, Gen. Rel. Grav. **41**, 2287 (2009); S. Basilakos, Mon. Not. R. Astron. Soc. **395**, 2347 (2009); J. S. Alcaniz et al., Phys. Lett. B **716**, 165 (2012)
15. N. Suzuki, D. Rubin, C. Lidman, G. Aldering, R. Amanullah, K. Barbary, L. F. Barrientos and J. Botyanszki *et al.*, Astrophys. J **746**, 85 (2012)
16. C. Blake et al., Mon. Not. Roy. Astron. Soc., **418**, 1707 (2011)
17. N. Sugiyama, Astrophys. J. Supp., **100**, 281 (1995)
18. D. L. Shafer and D. Huterer, Phys.Rev. D. **89**, 063510 (2014)
19. H. Akaike, IEEE Transactions of Automatic Control, **19** (1974) 716; N. Sugiura, Communications in Statistics A, Theory and Methods, **7** (1978) 13.
20. D. J. Eisenstein and W. Hu, Astrophys. J., **496**, 605 (1998)
21. H. A. Borges, S. Carneiro, J. C. Fabris, Phys. Rev. D. **78** 123522, (2008); H. A. Borges, S. Carneiro, J. C. Fabris and C. Pigozzo, Phys. Rev. D., **77**, 043513, (2008)
22. P.J.E. Peebles, “Principles of Physical Cosmology”, Princeton University Press, Princeton New Jersey (1993)
23. E. V. Linder and A. Jenkins, Mon. Not. Roy. Astron. Soc., **346**, 573 (2003)
24. V. Silveira and I. Waga, Phys. Rev. D., **50**, 4890 (1994)
25. L. Wang and P. J. Steinhardt, Astrophys. J., **508**, 483 (1998)
26. S. Nesseris and L. Perivolaropoulos, Phys. Rev. D., **77**, 023504 (2008)
27. S. Basilakos, S. Nesseris and L. Perivolaropoulos, Phys. Rev. D., **87**, 123529 (2013)
28. E. Macaulay, I. K. Wehus and H. K. Eriksen, Phys. Rev. Lett., **111**, 161301 (2013); S. Basilakos, [arXiv1412.2234]
29. N. Chandrachani Devi, H. A. Borges, S. Carneiro and J. S. Alcaniz, Mon. Not. Roy. Astron. Soc., **in press**, (arXiv:1407.1821)
30. W.H. Press and P. Schechter, Astrophys. J. **187**, 425 (1974)
31. V. Eke, S. Cole & C. S. Frenk, Mon. Not. Roy. Astron. Soc., **282**, 263, (1996)
32. A. Jenkins, et al., Mon. Not. Roy. Astron. Soc., **321**, 372 (2001)
33. L. Marassi and J. A. S. Lima, Int. J. Mod. Phys. D **13**, 1345 (2004); **ibidem**, IJMPD **16**, 445 (2007)
34. D. Reed, R. Bower, C. Frenk, A. Jenkins, and T. Theuns, MNRAS **374**, 2 (2007)
35. N. N. Weinberg and M. Kamionkowski, Astrophys. J., **341**, 251 (2003)
36. C. Fedeli, L. Moscardini, and S. Matarrese, Mon. Not. Roy. Astron. Soc., **397**, 1125 (2009)
37. S. Basilakos, M. Plionis and J. Solà, Phys. Rev. D., **82**, 083512 (2010)
38. O. Lahav, P. B. Lilje, J. R. Primack, & M. J. Rees, Mon. Not. Roy. Astron. Soc., **251**, 128, (1991)
39. S. Basilakos, Astrophys. J., **590**, 636, (2003)
40. C. Horellou & J. Berge, Mon. Not. Roy. Astron. Soc., **360**, 1393, (2005)
41. I. Maor, & O. Lahav, Journal of Cosmology and Astroparticle Physics, **7**, 3, (2005)
42. W. J. Percival, Astronomy & Astrophysics, **443**, 819, (2005)
43. P. Wang, Astrophys. J., **640**, 18, (2006)
44. D. F. Mota JCAP **09**, 006 (2008)

45. S. Basilakos, & N. Voglis, *Mon. Not. Roy. Astron. Soc.*, **374**, 269, (2007); S. Basilakos, J. C. Sanchez, L. Perivolaropoulos, *Phys. Rev. D.*, **80**, 3530, (2009)
46. F. Pace, J.-C. Waizmann and M. Bartelmann, *Mon. Not. Roy. Astron. Soc.*, **406**, 1865 (2010)